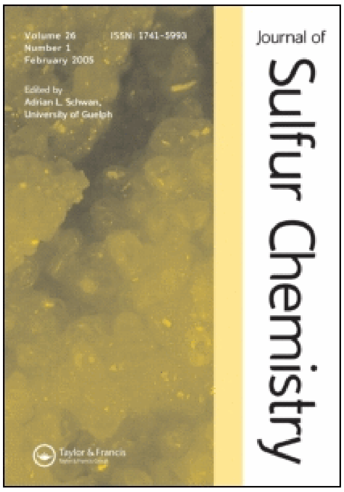

## Journal of Sulfur Chemistry

Publication details, including instructions for authors and subscription information:
http://www.informaworld.com/smpp/title~content=t713926081

# *Ab initio* investigations of the equilibria between trichlorothioacetyl chloride, tetrachlorothiirane, and trichloroethenesulfenyl chloride, their reactants and decomposition products

Kim V. Pedersen[a]; Henrik Christensen[a]; Irene Shim[a]; Alexander Senning[a]
[a] Department of Chemistry, Technical University of Denmark, Lyngby, Denmark

**To cite this Article** Pedersen, Kim V. , Christensen, Henrik , Shim, Irene and Senning, Alexander(2004) '*Ab initio* investigations of the equilibria between trichlorothioacetyl chloride, tetrachlorothiirane, and trichloroethenesulfenyl chloride, their reactants and decomposition products', Journal of Sulfur Chemistry, 25: 2, 111 — 123

**To link to this Article: DOI:** 10.1080/17415990410001680923

**URL:** http://dx.doi.org/10.1080/17415990410001680923

*J. Sulfur Chemistry*
Vol. 25, Nos. 2–3, April–June 2004, 111–123

Taylor & Francis
Taylor & Francis Group

RESEARCH ARTICLE

# *Ab initio* investigations of the equilibria between trichlorothioacetyl chloride, tetrachlorothiirane, and trichloroethenesulfenyl chloride, their reactants and decomposition products

KIM V. PEDERSEN, HENRIK CHRISTENSEN, IRENE SHIM* and
ALEXANDER SENNING

Department of Chemistry, Technical University of Denmark, Building 207,
DK-2800 Kgs, Lyngby, Denmark

(*Received 10 November 2003; In final form 22 January 2004*)

Trichlorothioacetyl chloride (**1**), tetrachlorothiirane (**2**), and trichloroethenesulfenyl chloride (**3**) and the equilibria between them have been investigated by *ab initio* Hartree–Fock (HF), Møller–Plesset second order perturbation (MP2) calculations, and by Gaussian-3 theory, G3 (MP2). Transition states of the isomerization reactions have been identified. Also investigated were possible reactions leading to the isomers and their possible decomposition products. The results show that the unobserved isomerization reactions are feasible.

*Keywords*: *Ab initio* HF, MP2, and G3 (MP2) calculations; Transition state; Activation energy; Trichlorothioacetyl chloride; Tetrachlorothiirane; Trichloroethenesulfenyl chloride

## 1. Introduction

Trichlorothioacetyl chloride (**1**) is stable only in the dark in dilute solutions, while tetrachlorothiirane (**2**) and trichloroethenesulfenyl chloride (**3**) are stable compounds at room temperature [1]. The possible chemical equilibria between the three compounds are shown in figure 1, but none of the suggested isomerization reactions have been observed experimentally [1].

Compound **1** photodimerizes to *trans*-2,4-bis(trichloromethyl)-2,4-dichloro-1,3-dithietane, *trans*-**4** (scheme 1) (2.1) [2]. In principle, **1** could also dimerize to *cis*-2,4-bis(trichloromethyl)-2,4-dichloro-1,3-dithietane, *cis*-**4** (2.2). The fluorine analog of **1**, trifluorothioacetyl fluoride,

---

* Corresponding author. E-mail: irene.shim@kemi.dtu.dk

*J. Sulfur Chemistry*
ISSN 1741-5993 print; ISSN 1741-6000 online
http://www.tandf.co.uk/journals
DOI: 10.1080/17415990410001680923

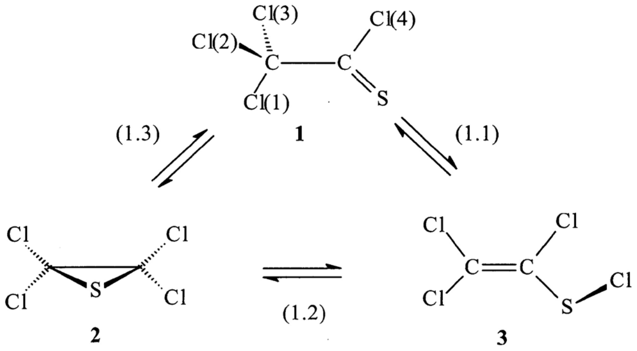

Figure 1. Possible equilibria between **1**, **2**, and **3**, along with the atom numbering of **1**.

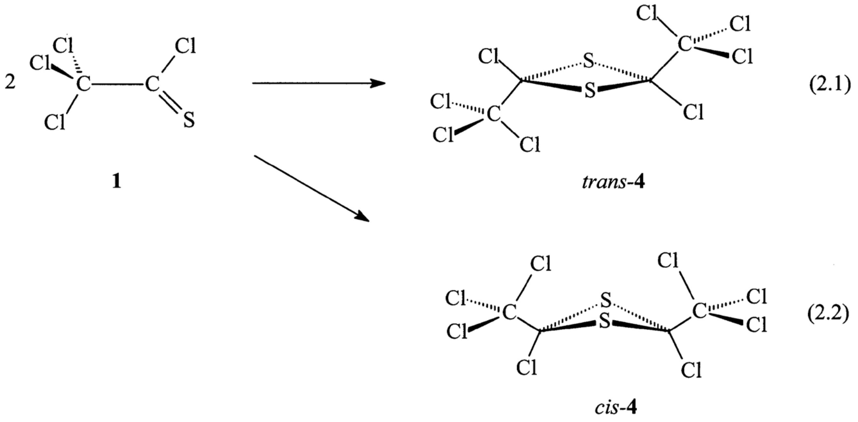

SCHEME 1 Dimerization reactions **1** → *trans*-**4** and **1** → *cis*-**4**.

photodimerizes by forming almost equal amounts of *trans*-2,4-bis(trifluoromethyl)-2,4-difluoro-1,3-dithietane and *cis*-2,4-bis(trifluoromethyl)-2,4-difluoro-1,3-dithietane [3].

Compound **1** has been synthesized (scheme 2), the initial reaction (3.1) is a radical reaction between tetrachloroethene (**5**) and sulfur dichloride (**6**) to produce pentachloroethanesulfenyl chloride (**7**) [4]. Compound **7** is then reduced with $SnCl_2$ to produce **1** [2], reaction (3.2).

Compound **2** can be synthesized from singlet dichlorocarbene (**10**) and thiophosgene (**11**) [scheme 3] [5], and can be desulfurized with phosphorus trichloride at room temperature to give **5** (scheme 4) [5]. As shown in scheme 5, compound **3** is prepared by chlorination of bis(1,2,2-trichloroethenyl) disulfide (**14**) [6].

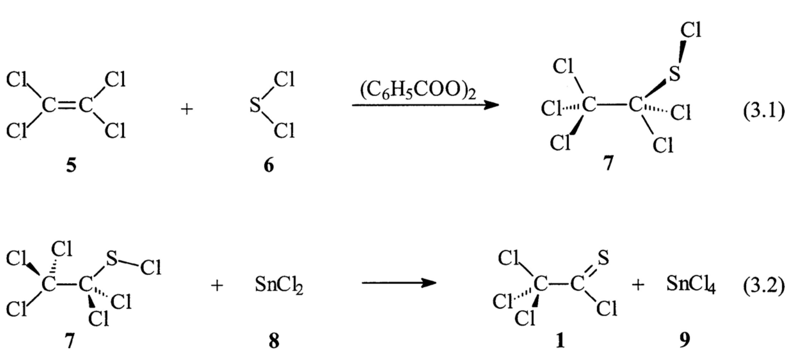

SCHEME 2 Synthesis of **1**.

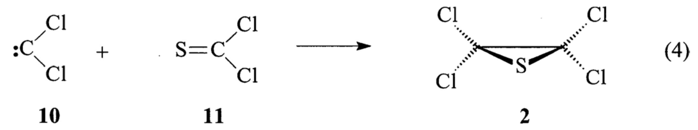

SCHEME 3 Synthesis of **2**.

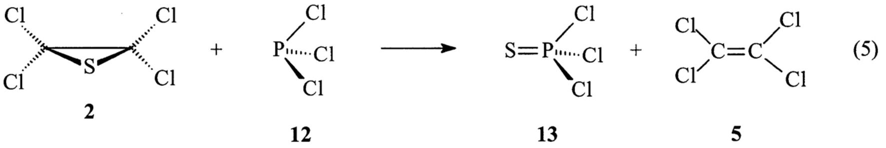

SCHEME 4 Desulfurization of **2**.

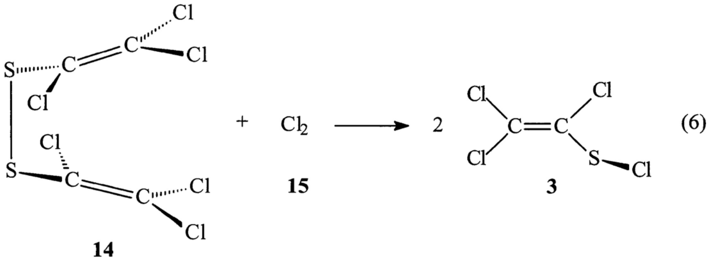

SCHEME 5 Synthesis of **3**.

## 2. Methods

In the present investigation the reactants and the products of reactions (1–6) have been studied by *ab initio* Hartree–Fock (HF) and Møller–Plesset second-order perturbation (MP2) calculations using the program SPARTAN [7]. In addition, Gaussian-3, G3 (MP2), calculations have been performed using Gaussian 98 [8]. Initially, the geometry of each molecule was optimized in HF calculations, and MP2 calculations were performed using the optimized geometries. HF and MP2 calculations have likewise been employed to elucidate the rotational barriers around the C—C bond in **1**, and around the C—S bond in **3**. HF, MP2, and G3 (MP2) calculations have been carried out to determine transition state structures for reactions (3.1) and (4) in which $SCl_2$ and $CCl_2$ are added to the double bonds in ethylene and thiophosgene, respectively. Furthermore, the reaction mechanisms involved in the possible isomerization reactions (1.1–1.3) have been investigated by HF, MP2, and G3 (MP2) calculations. The transition state structures have been identified by one negative eigenvalue of the Hessian matrix. These negative eigenvalues define reaction paths, and by following these paths it has been verified that the reaction paths identified connect the reactants with the products. Mulliken population analyses have been performed for both the stable molecules and the transition state structures.

The effects of the basis sets have been elucidated in HF calculations by determining the optimized geometries for **1** using five basis sets ranging from 3-21G(*) to 6—311 + G*. The results are presented in table 1. Also included are the structural data obtained by geometry optimization using full MP2 calculations. This method of optimization is employed as part of the G3 (MP2) calculations. The calculations show that the structural data of **1** are not very sensitive to the basis set used. Excluding the smallest basis set, 3-21G(*), the bond lengths deviate by, at most, 0.005 Å and the angles by 0.4°. In the present work HF and MP2 calculations were performed using the basis set 6-31G* for the atoms C, S and Cl. However, for the reactions involving the tin atom, the basis set 3-21G(*) was used.

Table 1. Optimized structures of **1** as resulting from HF calculations using various basis sets. Aslo included are the results obtained in full MP2 calculations using the basis set 6-31G*.

| | HF | | | | | MP2 (optimized, full) |
|---|---|---|---|---|---|---|
| | 3-21G(*) | 6-31G* | 6-31 + G* | 6-311G* | 6-311 + G* | 6-31G* |
| Energy (a.u.) +2300 a.u. | −0.50945 | −11.09947 | −11.10284 | −11.23655 | −11.24709 | −12.08420 |
| C(1)–S (Å) | 1.583 | 1.588 | 1.589 | 1.585 | 1.586 | 1.608 |
| C(1)–Cl(4) (Å) | 1.741 | 1.731 | 1.731 | 1.734 | 1.735 | 1.735 |
| C(1)–C(2) (Å) | 1.546 | 1.550 | 1.549 | 1.548 | 1.548 | 1.546 |
| C(2)–Cl(1) (Å) | 1.773 | 1.762 | 1.762 | 1.763 | 1.763 | 1.761 |
| C(2)–Cl(2), C(2)–Cl(3) (Å) | 1.788 | 1.776 | 1.776 | 1.776 | 1.777 | 1.776 |
| S–C(1)–Cl(4) (°) | 122.0 | 121.7 | 121.6 | 121.4 | 121.5 | 122.5 |
| S–C(1)–C(2) (°) | 126.0 | 125.9 | 125.8 | 126.2 | 126.1 | 125.8 |
| Cl(4)–C(1)–C(2) (°) | 112.1 | 112.5 | 112.5 | 112.4 | 112.4 | 111.8 |
| C(1)–C(2)–Cl(1) (°) | 112.3 | 112.4 | 112.4 | 112.3 | 112.4 | 111.8 |
| Cl(2)–C(2)–Cl(3) (°) | 109.7 | 109.9 | 109.9 | 109.9 | 109.9 | 110.2 |
| C(1)–C(2)–Cl(2), C(1)–C(2)–Cl(3) (°) | 108.9 | 108.8 | 108.8 | 108.8 | 108.8 | 108.5 |
| Cl(2)–C(2)–Cl(1), Cl(3)–C(2)–Cl(1) (°) | 108.5 | 108.4 | 108.5 | 108.5 | 108.5 | 108.5 |
| S–Cl(4) Å | 2.908 | 2.899 | 2.899 | 2.895 | 2.898 | 2.931 |
| S–Cl(1) Å | 3.167 | 3.169 | 3.170 | 3.173 | 3.174 | 3.159 |

The total energies of the compounds investigated are presented in the Appendix. The results derived in MP2 and G3 (MP2) calculations for the stable species are shown in table AI. Correspondingly, the energies of the transition state structures identified are presented in table AII.

## 3. Results and discussions

The discussion below is based on the structures obtained in full MP2 optimizations, and the Mulliken populations are those derived using the basis set 6-31G*.

### 3.1 *Reactions (2)–(6)*

Table 2 presents the reaction energies for reactions (2)–(6) as derived in MP2 and G3 (MP2) calculations. Also included are the reaction enthalpies and Gibbs energies obtained in the G3 (MP2) calculations. Table 2 shows that all the reactions studied are exothermic. The MP2 results, $\Delta E$, are from single point calculations using the HF optimized geometries, and $\Delta E_\mathrm{e}$ are from optimizations performed in full MP2 calculations. The deviation between the $\Delta E$ and $\Delta E_\mathrm{e}$ amounts to at most 7 kJ mol$^{-1}$. The discrepancies between the $\Delta E_\mathrm{e}$s derived in MP2 and in G3 (MP2) calculations are due to both the basis set corrections and the correlation energies. In Gaussian-3 theory various empiric and non-empiric corrections are included to derive the final results. Thus, the zero-point energy is based on the frequencies derived in HF calculations, but scaled by the factor 0.8929. Furthermore, the ideal gas law is used to derive the enthalpies and the Gibbs energies. While the $\Delta H$s differ at most by 2 kJ mol$^{-1}$ from the $\Delta E_0$s, and by at most 7 kJ mol$^{-1}$ from the $\Delta E_\mathrm{e}$s, the $\Delta G$s differ considerably from $\Delta E_\mathrm{e}$ and $\Delta E_0$. This is mostly attributed to differences in entropy, which is especially evident when the reactions result in a change in the number of molecules, as in reactions (2.1), (2.2), (3.1) and (4).

The thermodynamically most stable isomer, **1**, is stable only in the dark. This is due to the dimerization that occurs according to reaction (2.1). The dimers of **1**, *trans*-**4** and *cis*-**4**, in reactions (2.1) and (2.2) are both thermodynamically stable relative to **1**, by 57 and 48 kJ mol$^{-1}$, respectively; *trans*-**4** is more stable than *cis*-**4**. The difference between their $\Delta E_\mathrm{e}$s is 10 kJ mol$^{-1}$, and between their $\Delta H_{298.15}$ and $\Delta G_{298.15}$s 9 kJ mol$^{-1}$. These results deviate from those of the fluorine analogs where the *cis* compound is more stable than the *trans* compound, but only by 1 kJ mol$^{-1}$ [9]. Results for the chlorine compounds, *trans*-**4** and *cis*-**4**, are consistent with the fact that only *trans*-**4** is observed in the dimerization reaction. Compound

Table 2. Reaction energies ($\Delta E$), enthalpies ($\Delta H$), and Gibbs energies ($\Delta G$) (kJ mol$^{-1}$) of reactions (2)–(6) as derived in MP2 and G3 (MP2) calculations.

| | MP2 6-31G* | | G3 (MP2) | | | |
|---|---|---|---|---|---|---|
| | HF geometry frozen core | MP2 geometry full | | | | |
| Reaction | $-\Delta E$ | $-\Delta E_e$ | $-\Delta E_e$ | $-\Delta E_0$ | $-\Delta H_{298.15}$ | $-\Delta G_{298.15}$ |
| 2.1 | 100 | 107 | 129 | 122 | 123 | 57 |
| 2.2 | 89 | 96 | 119 | 113 | 114 | 48 |
| 3.1[a] | 89 | 91 | 84 | 80 | 81 | 28 |
| 3.2 | (295)[b] | | | | | |
| 4 | 295 | 300 | 254 | 242 | 244 | 187 |
| 5 | 53 | 56 | 73 | 71 | 70 | 73 |
| 6 | 22 | 17 | 11 | 11 | 13 | 21 |

[a] Dihedral angle C–C–S–Cl, $\Theta = 84.3°$. [b] Basis set 3-21G(*).

*trans*-**4** has a planar 1,3-dithietane ring. According to both HF and MP2 calculations on 1,3-dithietane the geometry of the 1,3-dithietane ring in *trans*-**4** is almost identical to that of the parent 1,3-dithietane. However, the 1,3-dithietane ring in *cis*-**4** is slightly puckered with one C atom 9.9° out of the plane formed by the other C atom and the two S atoms. In *trans*-**4** the distance between the closest Cl atoms in the *cis* position, *i.e.* one bound directly to the 1,3-dithietane ring and one in the trichloromethyl group, is 3.640 Å. This distance lies between those observed in *cis*-**4**, for which the bending of the 1,3-dithietane ring results in the two closest Cl atoms in the *cis* trichloromethyl groups being 3.440 Å apart, while the two Cl atoms directly bound to the 1,3-dithietane ring are 3.840 Å apart.

Investigations of the reactions leading to **1**, (3.1) and (3.2), show that reaction (3.1) producing **7** is exothermic. For this reaction the activation energy, the enthalpy and the Gibbs energy, $\Delta E_e^{\ddagger}$, $\Delta H_{298.15}^{\ddagger}$, and $\Delta G_{298.15}^{\ddagger}$, were derived as 155, 154, and 198 kJ mol$^{-1}$, respectively. The reduction of **7** with $SnCl_2$ produces **1**.

The most exothermic reaction studied is reaction (4), which leads to **2**. For this reaction the activation energy, $\Delta G_{298.15}^{\ddagger}$, is determined as only 32 kJ mol$^{-1}$, implying that the reaction will proceed to form **2** when the correct orientation of the reactants is achieved.

Phosphorus trichloride reacts exothermically with **2** to produce tetrachloroethene (**5**) [reaction (5); $\Delta G_{298.15} = 73$ kJ mol$^{-1}$].

Chlorination of **14** in reaction (6) leads to **3** (scheme 5). The energy released in this reaction amounts to 21 kJ mol$^{-1}$. Compound **14** consists of two facing $-SClC{=}CCl_2$ groups; the dihedral angle C−S−S−C has been determined as 74.3°, and the S−S bond length is 2.08 Å.

### 3.1.1 *Transition state structures of the addition reactions (3.1) and (4).*

Reactions (3.1) and (4) represent additions to double bonds. In (3.1) $SCl_2$ is added to the C=C double bond of ethylene, and in (4) $CCl_2$ is added to the C=S double bond of thiophosgene.

For reaction (3.1) the transition structure presented in figure 2 was identified. The displacement vectors of the imaginary frequency show that the distance between one C atom of tetrachloroethene and the S atom of sulfur dichloride decreases considerably during the vibration defined by the imaginary frequency. The incipient bond is formed between one C atom of tetrachloroethene and the S atom of sulfur dichloride by interactions between the HOMO of **5** and the LUMO of **6**.The S and the C atoms that become bound in **7** are 1.99 Å apart. This distance is approaching the final bond length of 1.84 Å in **7**. The distance between the chlorine atom and the C atom to which it becomes bound in **7** is 2.75 Å, *i.e.* considerably longer than the final bond length 1.77 Å in **7**. The chlorine atom has acquired a charge of −0.44 e.

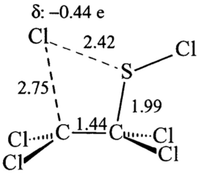

Figure 2. Transition state in reaction (3.1), **TS** (3.1); distances in Å.

The transition state structure for reaction (4) as obtained in MP2 (full) calculations is shown in figure 3. The optimized distance between the C atom of $CCl_2$ and the S atom of $S{=}CCl_2$ is 2.00 Å when derived in HF calculations, but this increases to 2.49 Å in MP2 (full) calculations. Consequently, further investigations are needed to fully clarify the nature of the interaction between $CCl_2$ and $S{=}CCl_2$. However, during the vibration defined by the imaginary frequency the C atom of **10** and the S atom of **11** approach each other, indicating that the structure represents an early transition state with an incipient bond between these two atoms. Altogether,

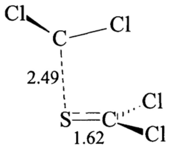

Figure 3. Transition state in reaction (4), **TS** (4); distances in Å.

only slight changes in the geometries of the interacting molecules have occurred. The $CCl_2$ molecule is in a plane almost parallel to that of the $S{=}CCl_2$ molecule, with the C−Cl bond and the S−C bonds almost parallel. The two C atoms are 3.20 Å apart, more than twice the final 1.50 Å in **2**, and the angle C−S−C is 105.1°. The reaction appears to be non-concerted.

### 3.2 *Rotational barriers of 1 and 3*

Rotational barriers around the C−C bond in **1**, and around the C−S bond in **3** have been investigated by optimizing the geometry subject to constraining the appropriate dihedral angle in HF calculations. Frozen core MP2 calculations were performed for the HF optimized geometries.

The rotational barrier of **1** is 13.2 kJ $mol^{-1}$. This is considerably larger than the barrier for the analogous fluorine compound (5.3 kJ $mol^{-1}$). The rotational barrier in **1** is, however, similar to that of ethane, and thus, at room temperature, there is essentially free rotation around the C−C bond in **1**.

The rotational barrier around the C−S bond in **3** (31.2 kJ $mol^{-1}$) shows that rotation around the C−S bond is hindered at room temperature. The most stable conformation of **3** has a dihedral angle C(2)−C(1)−S−Cl(1) of 111°. The sizable rotational barrier is connected with the change of symmetry from $C_1$ to $C_s$. Thus, in the $C_s$ species the HOMO is anti-bonding between the C−C bonding $\pi$ orbital and a lone pair on the S atom. As the symmetry changes the HOMO becomes a delocalized bonding orbital extending over the two C atoms and over the S atom. Figure 4 shows the rotational barrier for **3** along with a definition of the dihedral angle.

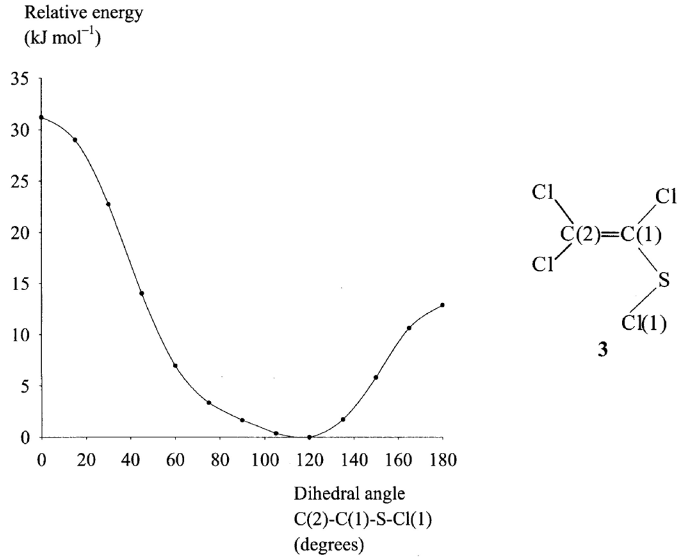

Figure 4. Rotational barrier around the C−S single bond in **3** as derived in MP2 calculations. Also shown is **3** with the dihedral angle C(2)−C(1)−S−Cl(1) equal to 0°.

The rotational barrier around the C—S bond in **3** (figure 4) is remarkably different from the corresponding potential for the fluorine analogue. The latter potential is much less asymmetric, with a barrier of 42.6 kJ mol$^{-1}$ at 180° and of 38.0 kJ mol$^{-1}$ at 0°, and the minimum is located at the dihedral angle 97°. Compound **3** appears to be stabilized in the planar geometries by electronic interaction between the negatively charged Cl atom attached to S and a slightly positively charged Cl atom attached to C. The stabilization is larger at a dihedral angle 180° than at 0°. At 180° the Cl—S group and the Cl atom are attached to the same C atom while at 0° the Cl—S group and the Cl atom are attached to neighbouring C atoms.

### 3.3 *Isomerization reactions 3 → 1, 3 → 2, and 2 → 1*

Simultaneously with the present work the fluorine analogs of the isomerization reactions (1.1–1.3) have been investigated [9].

Table 3 shows the relative energies of the isomers, **1-3** with three characteristic conformations of **3**. The thermodynamically most stable compound is **1**, but the energy differences are small, much smaller than those of the corresponding fluorine compounds [9]. The results of the G3 (MP2) calculations reveal that **3** is only 5 kJ mol$^{-1}$ less stable than **1**. The lowering of the energy of **3** relative to **1** is especially due to the basis set corrections and the correlation energy included in the G3 (MP2) method.

Transition state structures for the isomerizations **3** → **1**, **3** → **2**, and **2** → **1** have been identified (schemes 6–8, respectively). Table 4 shows the activation energies resulting from MP2 and G3 (MP2) calculations.

The energies presented in table 4 indicate that it is possible for **3** and **2** to rearrange into **1**, but the activation energies of the isomerization reactions are relatively high, *i.e.* 189 and 237 kJ mol$^{-1}$, respectively. Compound **3** can in principle also rearrange into **2**, but this reaction is unlikely since the energy barrier is 191 kJ mol$^{-1}$, comparable to that of the rearrangement to **1**, and, in addition, this reaction is endothermic by 17 kJ mol$^{-1}$.

The transition state structure involved in the rearrangement **3** to **1**, **TS** (1.1) scheme 6, is appreciably polar. According to the Mulliken population analysis the Cl atom that is attached to S in **3** and to C in **1** has acquired the charge −0.50 e. The distance between this Cl atom and the S atom has increased from 2.05 Å in **3** to 2.81 Å in **TS** (1.1). Thus, the Cl atom is closer to the C atom to which it finally becomes attached, *i.e.* 2.70 Å, than to the S atom where it was originally attached, but the distance between Cl and C is still much larger than the final 1.76 Å in **1**. The C—S distance has decreased from 1.74 Å in **3** to 1.65 Å in **TS** (1.1). This is close to its final value of 1.61 Å in **1**. The C atoms are 1.43 Å apart, which is in between the 1.36 Å of **3** and the 1.55 Å of **1**. The dihedral angle C—C—S—Cl in **TS** (1.1) is 56.9°. Although the transition state structure indicates that the moving Cl atom is only weakly bound, the displacement vectors defined by the imaginary frequency show that the Cl atom during this vibration approaches the C atom to which it becomes bound in **1**.

The reaction appears to be initiated by rotation around the C—S bond, thereby overcoming part of the activation energy. The reaction then proceeds as electrons flow from the C=C double bond to the C—S single bond, resulting in one weakly bound Cl atom with a negative charge that attacks the C atom to which it finally becomes bound.

The transition state, **TS** (1.2), identified for the isomerization **3** → **2** is shown in scheme 7. According to Mulliken population analysis the transition state is polar with a charge of −0.69 e on the Cl atom that moves from S to C. The moving Cl atom is 2.71 Å from C and 2.76 Å from S, but the displacement vectors defined by the imaginary frequency show that the Cl atom during this vibration is approaching the C atom to which it becomes bound in **2**.

The activation energies of reactions **3** → **2** and **3** → **1** are similar, 191 and 189 kJ mol$^{-1}$, respectively. This is consistent with the changes of the molecular geometries that have occurred. Thus, it is noted that in both transition state structures the C—C distance is 1.43 Å and the C—S

Table 3. Relative energies ($\Delta E$), enthalpies ($\Delta H_{298.15}$), and Gibbs energies ($\Delta G_{298.15}$) (kJ mol$^{-1}$) of the $C_2Cl_4S$ isomers **1**–**3** as derived in MP2 and G3 (MP2) calculations.

| | | | MP2 6-31G* | | | | | |
|---|---|---|---|---|---|---|---|---|
| | | | HF geometry frozen core | MP2 geometry full | G3 (MP2) | | | |
| Isomer | Name | Symmetry | $\Delta E$ | $\Delta E_e$ | $\Delta E_e$ | $\Delta E_0$ | $\Delta E_{298.15}$ | $\Delta E_{298.15}$ |
| **1** | trichlorothioacetyl chloride | $C_s$ | 0 | 0 | 0 | 0 | 0 | 0 |
| **2** | tetrachlorothiirane | $C_{2v}$ | 11 | 11 | 17 | 18 | 17 | 22 |
| **3**(1) | trichloroethenesulfenyl chloride | $C_1$ | 41 | 39 | 9 | 8 | 9 | 5 |
| **3**(2)[a] | trichloroethenesulfenyl chloride | $C_s$ | 72 | | | | | |
| **3**(3)[b] | trichloroethenesulfenyl chloride | $C_s$ | 54 | | | | | |

[a] Dihedral angle C(2)–C(1)–S–Cl(1) is 0°, see Figure 4. [b] Dihedral angle C(2)–C(1)–S–Cl(1) is 180°, see Figure 4.

Table 4. Activation energies, ($\Delta E^{\ddagger}$), enthalpies ($\Delta H^{\ddagger}_{298.15}$), and Gibbs energies ($\Delta G^{\ddagger}_{298.15}$) (kJ mol$^{-1}$) derived in MP2 and G3(MP2) calculations for the isomerization reactions between the $C_2Cl_4S$ isomers.

| | | MP2 6-31G* | | G3 (MP2) | | | |
|---|---|---|---|---|---|---|---|
| | Transition | HF geometry frozen core | MP2 geometry full | | | | |
| Reaction | state | $\Delta E^{\ddagger}$ | $\Delta E^{\ddagger}_{e}$ | $\Delta E^{\ddagger}_{e}$ | $\Delta E^{\ddagger}_{0}$ | $\Delta H^{\ddagger}_{298.15}$ | $\Delta G^{\ddagger}_{298.15}$ |
| **3** → **1** | TS (1.1) | 201 | 194 | 191 | 185 | 184 | 189 |
| **3** → **2** | TS (1.2) | 198 | 194 | 193 | 188 | 187 | 191 |
| **2** → **1** | TS (1.3) | 297 | 275 | 248 | 243 | 244 | 237 |
| 3.1 | TS (3.1) | 184 | 181 | 155 | 153 | 154 | 198 |
| 4 | TS (4) | −40 | −9 | −17 | −13 | −14 | 32 |

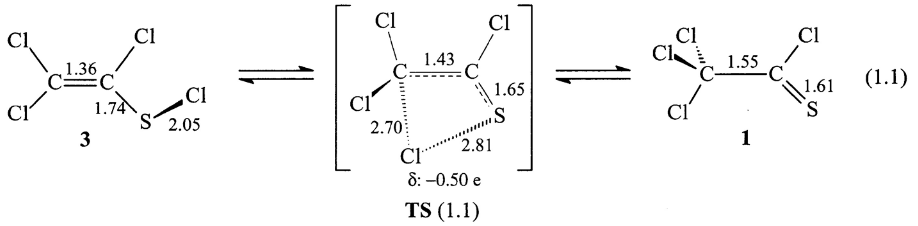

SCHEME 6 Transition state structure in the isomerization **3** → **1**; distances in Å.

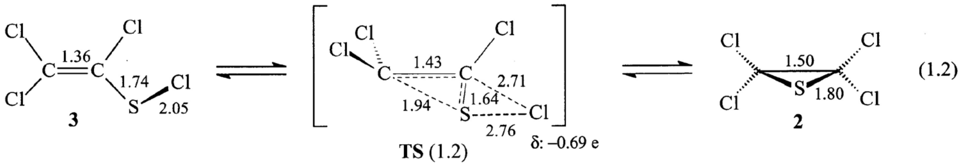

SCHEME 7 Transition state structure in the isomerization **3** → **2**; distances in Å.

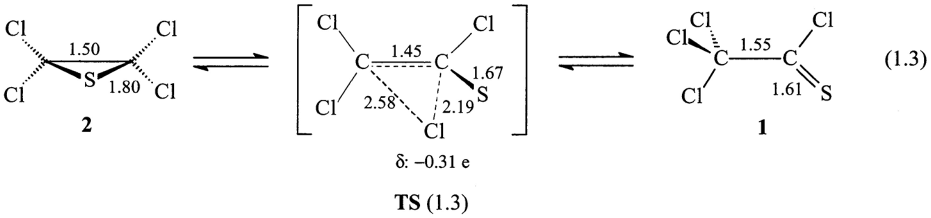

SCHEME 8 Transition state structure in the isomerization **2** → **1**; distances in Å.

distance is 1.65 Å in **TS** (1.1) and 1.64 Å in **TS** (1.2). To reach the transition state in reaction (1.2) the C=C double bond is partly broken while the C−S bond has acquired some double bond character. In addition, the C−C−S angle has changed from 125.8° in **3** to 78.2° in **TS** (1.2). Altogether, the moving Cl atom appears to be weakly bound, and this reaction could possibly occur through an ionic intermediate.

The transition state in reaction (1.3) [**TS** (1.3), scheme 8] indicates that the S atom is moving towards one C atom while the Cl atom is moving towards the other C atom in an apparent one-step process. In the transition state the S atom and the closest C atom are 1.67 Å apart. This is approaching the final C−S distance in **1** (1.61 Å). In the transition state the distance between the moving Cl atom and the C atom where it was originally attached in **2** has increased from 1.75 to 2.19 Å, but it is still 2.58 Å from the C atom to which it becomes attached in **1** (bond length 1.76 Å). According to the Mulliken population analysis the moving Cl atom has acquired the charge −0.31 e. Thus, the transition state **TS** (1.3) is the least polar of the three transition states identified. The C−C distance (1.45 Å) is shorter than that of both **2** (1.50 Å) and **1** (1.55 Å), indicating that the C−C bond has acquired some double bond character as the C−S bond is broken. According to the displacement vectors defined by the imaginary frequency it appears that the reaction proceeds from the transition state as the Cl atom slides along the C−C bond.

All the transition states identified are appreciably polar, but the energies of the proposed transition states are lower than the totally ionic states by 477, 415 and 479 kJ mol$^{-1}$ for the transition states **TS** (1.1), **TS** (1.2) and **TS** (1.3), respectively. Polar solvents will stabilize both the polar transition states and, especially, the totally ionic states. The influence of solvents has not been the subject of the present investigation, and thus further studies are needed to clarify this matter.

The structures of the transition states identified for reactions (1.1–1.3) strongly resemble those identified for the analogue reactions of the fluorine compounds.

Our calculations are consistent with the fact that all three isomers, **1**–**3**, exist as stable compounds. Furthermore, the isomerization reactions (1.1–1.3), which have not been observed experimentally, are feasible.

## Acknowledgments

The authors thank the Technical University of Denmark and the Danish Center for Scientific Computing for providing computational resources.

## References

[1] Senning, A. and El-Kousy, S., 1997, *Sulf. Rep.*, **20**, 197.

[2] Laifa, E.-A., Abdel-Megeed, M. F., Ghattas, A.-B. A. G., Jensen, B. and Senning, A., 1987, *Sulf. Lett.*, **5**, 155.

[3] Middleton, W. J., Howard, E. G. and Sharkey, W. H., 1965, *J. Org. Chem.*, **30**, 1375.

[4] Senning, A., Chevallier, M.-A. and Jensen, B., 1985, *Sulf. Lett.*, **3**, 177.

[5] Seyferth, D., Tronich, W., Marmor, R. S. and Smith, W. E., 1972, *J. Org. Chem.*, **37**, 1537.

[6] Weil, E. D., Smith, K. J. and Geering, E. J., 1968 (Hooker Chemical Corp.), U.S. Pat. 3,366,643.

[7] SPARTAN, version 5.1.3 X11, Wavefunction Inc, Suite 370, Irvine, CA.

[8] Frisch, M. J., Trucks, G. W., Schlegel, H. B., Scuseria, G. E., Robb, M. A., Cheeseman, J. R., Zakrzewski, V. G., Montgomery Jr., J. A., Stratmann, R. E., Burant, J. C., Dapprich, S., Millam, J. M., Daniels, A. D., Kudin, K. N., Strain, M. C., Farkas, O., Tomasi, J., Barone, V., Cossi, M., Cammi, R., Mennucci, B., Pomelli, C., Adamo, C., Clifford, S., Ochterski, J., Petersson, G. A., Ayala, P. Y., Cui, Q., Morokuma, K., Rega, N., Salvador, P., Dannenberg, J. J., Malick, D. K., Rabuck, A. D., Raghavachari, K., Foresman, J. B., Cioslowski, J., Ortiz, J. V., Baboul, A. G., Stefanov, B. B., Liu, G., Liashenko, A., Piskorz, P., Komaromi, I., Gomperts, R., Martin, R. L., Fox, D. J., Keith, T., Al-Laham, M. A., Peng, C. Y., Nanayakkara, A., Challacombe, M., Gill, P. M. W., Johnson, B., Chen, W., Wong, M. W., Andres, J. L., Gonzalez, C., Head-Gordon, M., Replogle, E. S. and Pople, J. A. Gaussian 98, Revision A.11.2, 2001, (Pittsburgh, PA: Gaussian, Inc.).

[9] Shim, I., Vallano-Lorenzo, S., Lisbona-Martin, P. and Senning, A., 2003, *J. Fluorine Chem.*, **124**, 99.

## Appendix

Total energies of the compounds investigated (tables AI and AII).

Table AI. Total energies (a.u.) of the stable compounds as derived in MP2 and G3 (MP2) calculations.

| | | | MP2 6-31G* | | G3 (MP2) | | | |
|---|---|---|---|---|---|---|---|---|
| | | | HF geometry frozen core | MP2 geometry full | | | | |
| Compound | Name | Symmetry | $E$ | $E_e$ | $E_e$ | $E_0$ | $H_{298.15}$ | $G_{298.15}$ |
| **1** | trichlorothioacetyl chloride | $C_s$ | −2312.02145 | −2312.08420 | −2312.83720 | −2312.82052 | −2312.81170 | −2312.85534 |
| **2** | tetrachlorothiirane | $C_{2v}$ | −2312.01739 | −2312.08012 | −2312.83068 | −2312.81377 | −2312.80522 | −2312.84694 |
| **3** | trichloroethenesulfenyl chloride | $C_1$ | −2312.00593 | −2312.06930 | −2312.83413 | −2312.81736 | −2312.80814 | −2312.85351 |
| *trans*-**4** | *trans*-2,4-bis(trichloromethyl)-2,4-dichloro-1,3-dithietane | $C_{2h}$ | −4624.08114 | −4624.20909 | −4625.72355 | −4625.68757 | −4625.67038 | −4625.73252 |
| *cis*-**4** | *cis*-2,4-bis(trichloromethyl)-2,4-dichloro-1,3-dithietane | $C_{2v}$ | −4624.07690 | −4624.20483 | −4625.71990 | −4625.68398 | −4625.66675 | −4625.72909 |
| **5** | tetrachloroethene | $D_{2h}$ | −1914.38774 | −1914.43979 | −1915.07930 | −1915.06394 | −1915.05648 | −1915.09521 |
| **6** | sulfur dichloride | $C_{2v}$ | −1316.81257 | −1316.84340 | −1317.24256 | −1317.23976 | −1317.23500 | −1317.26698 |
| **7** (1)[a] | pentachloroethanesulfenyl chloride | $C_1$ | −3231.23439 | −3231.31788 | −3231.35395 | −3232.33414 | −3232.32225 | −3232.37283 |
| **7** (2)[b] | pentachloroethanesulfenyl chloride | $C_1$ | −3231.22054 | −3231.31831 | −3231.35336 | −3232.33355 | −3232.32164 | −3232.37239 |
| **10** | dichlorocarbene | $C_{2v}$ | −957.08627 | −957.11064 | −957.44606 | −957.44198 | −957.43762 | −957.46769 |
| **11** | thiophosgene | $C_{2v}$ | −1354.81870 | −1354.85532 | −1355.28781 | −1355.27978 | −1355.27459 | −1355.30800 |
| **12** | phosphorus trichloride | $C_{3v}$ | −1719.70379 | −1719.74547 | −1720.25688 | −1720.25208 | −1720.24597 | −1720.28141 |
| **13** | thiophosphoryl chloride | $C_s$ | −2117.35362 | −2117.40695 | −2118.03622 | −2118.02877 | −2118.02149 | −2118.06090 |
| **14** | bis(1,2,2-trichloroethenyl) disulfide | $C_s$ | −3704.83220 | −3704.94054 | −3706.19779 | −3706.16546 | −3706.15002 | −3706.21227 |
| **15** | chlorine | | −919.17116 | −919.19122 | −919.46617 | −919.46495 | −919.46144 | −919.48674 |

[a] Dihedral angle C−C−S−Cl is 84.3 °. [b] Dihedral angle C−C−S−Cl is 180.0 °.

Table AII. Total energies (a.u.) of all the transition state structures as derived in MP2 and G3 (MP2) calculations; also included are the zero points energies and the imaginary frequencies obtained in HF calculations.

| Transition state structure | MP2 6-31G* |  | G3 (MP2) |  |  |  | Zero-point energies (a.u.) | Imaginary frequency (cm$^{-1}$) |
|---|---|---|---|---|---|---|---|---|
|  | HF geometry frozen core | MP2 geometry full | $E_e$ | $E_0$ | $H_{298,15}$ | $G_{298,15}$ |  |  |
| **TS** (1.1) | −2311.93036 | −2311.99549 | −2312.76052 | −2312.74566 | −2312.73677 | −2312.78067 | 0.014868 | 600 |
| **TS** (1.2) | −2311.90421 | −2311.97522 | −2312.73634 | −2312.72113 | −2312.71217 | −2312.75682 | 0.015216 | 230 |
| **TS** (1.3) | −2311.92928 | −2311.99540 | −2312.76126 | −2312.74680 | −2312.73800 | −2312.78135 | 0.014460 | 418 |
| **TS** (3.1) | −3231.13041 | −3231.21434 | −3232.26286 | −3232.24560 | −3232.23300 | −3232.28669 | 0.017259 | 405 |
| **TS** (4) | −2311.92028 | −2311.96944 | −2312.74037 | −2312.72687 | −2312.71761 | −2312.76346 | 0.013497 | 362 |